532.525:536.242 Paper No. 139-12

Heat Transfer of the Impinging Round Water Jet in the Interference Zone of Film Flow along the Wall*

By Seikan ISHIGAI**, Shigeyasu NAKANISHI***, Minoru MIZUNO**** and Toyoo IMAMURA*****

A round jet of water impinging vertically on a horizontal plane forms a thin film flowing radially which later turns into an ordinary flow after passing through a hydraulic jump region. Hydrodynamic and heat transfer characteristics of two domains of the flow are investigated experimentally. The one domain is the jump region and the other is the interfering films of two equal jets. These two domains have several properties similar to each other because they are both interference zones of two flow regions. The radial location of the interference is found to be an important factor in the hydraulic and thermal properties of the interference region. The film of the jet flow is measured and analysed. It is found that different behaviors of the interference zone are characterized by the film Froude number and the Reynolds number taking the radius from the center of the jet as the representative length.

1. introduction

A cooling method using the water film formed by an impinging round jet of water possesses locally high heat transfer coefficients. But this method has a defect in that the cooling effect becomes lower at large radius measured from the center of the jet.[1] There are two means to remedy this defect. The one is a method which induces a hydraulic jump at the location where heat transfer coefficient is low. The other is a method which utilizes several water jets. These two methods have several properties similar to each other because they are both interference regions of film flow with other flow. When several water jets are impinging on the horizontal plate, an interference region of the water films occurs. The hydraulic jump occurs by the interference of the film flow with the water at the periphery of the plate. To know hydrodynamic and heat transfer characteristics of these interference regions, it is necessary to know the hydrodynamic characteristics of the film flow without interference region.

Watson analysed approximately this film flow by using the momentum integral equation.[2] Nagai et al. measured the thickness of the film flow.[3] But discrepancy between them is considerably large.

In this paper at first the film flow formed by an impinging jet on the horizontal plane is described. Subsequently the hydrodynamic and heat transfer characteristics of the two interference regions of the film flow are described. The one is the hydraulic jump and the other is the interference region formed by two equal impinging jets.

NOMENCLATURE

Fr	:	Film Froude number ($=u_m/\sqrt{g\delta}$)
H	:	Distance from the nozzle outlet to the test plate
K_1	:	Constant
K_2	:	Constant
L	:	Length of the nozzle
P	:	Jet pitch
Q	:	Volumetric flow rate
Rer	:	Reynolds number ($=u_i r/\nu$)
Rer_j	:	Reynolds number ($=u_j r_j/\nu$)
Recr	:	Critical value for Rer
Reδ	:	Reynolds number ($=u_m\delta/\nu$)
U_m	:	Flow velocity after hydraulic jump
d_o	:	Inner diameter of the nozzle
f	:	Dimension-less velocity profile
g	:	Gravitational acceleration
h_o	:	Heat transfer coefficient ($=q/(t_w-t_o)$)
q	:	Heat flux
r	:	Radius measured from the center of the jet
r_a	:	Radius where boundary layer thickness equals to film thickness
r_j	:	Radius of jump
r^*	:	Dimensionless radius
r_a^*	:	Dimensionless radius corresponding to r_a
t_o	:	Jet temperature
t_w	:	Backside temperature of heating plate

* Received 10th June, 1974

** Proffessor, Fuculty of Engineering, Osaka University.
*** Associate Proffessor, Fuculty of Engineering, Osaka University.
**** Assistant Proffessor, Fuculty of Engineering, Osaka University.
***** Kanegafuchi Kagaku Kogyo,

: Surface temperature of heating plate
: Flow velocity
: Jet velocity at impinging point ($= \sqrt{u_o^2+2gH}$)
: Jet velocity at nozzle outlet
: Mean velocity in water film
: Velocity at free surface of water film
: Coordinate
: Coordinate
: Thickness of water film
: Thickness of water film before hydraulic jump
: Thickness of water film after hydraulic jump
: Boundary layer thickness
: Thickness of heating plate
: Dimensionless film thickness
: Thermal conductivity of heating plate
: Dimensionless coordinate
: Kinematic viscosity

2. Experimental apparatus and procedures

2.1 Experiments with a single jet

Flow system of the water for a jet is shown in Fig.1. The water is pumped up from the tank through the cooler and introduced into the inlet pipe to the nozzle. The inlet pipe is 3 inches in diameter and 7 m in length and made of vinyl chloride. The lower end of this pipe is narrowed to a corn-shape whose vertical angle is about 30 degrees and a glass pipe for the nozzle is connected smoothly to the end of the pipe. The length of the glass pipe is desirably as short as possible in order to obtain a jet which has uniform velocity distribution over its cross section. But when this length is too short, vena contracta occurs. In the experiments the glass pipes whose length are 3 times their diameter were used. On the other hand if the pipe is very long, the developed velocity profile in the pipe is established. It is known that for the turbulent flow $50d_o$ is enough to establish this profile.[4] Experiments were performed also with long nozzle ($L = 50d_o$) to examine the influence of this velocity profile on the film flow.

The brass plate whose diameter was 500 mm was used as the test plate to measure the thickness of the film. The film thickness was measured with a micrometer equipped with a needle. Voltage was applied between this needle and the test plate. The osciloscope was used to detect the voltage change caused when the needle contacted with water surface. When the water surface was wavy, the contact time was defined as the time within which the needle contacted with the water surface. In this case the film thickness was evaluated as the value whose contact time was 50 % of the full time.

The radius of a hydraulic jump was changed by changing the height of a weir set around the test plate. The weir was made of rubber and its height was changed between 0 and 10 mm.

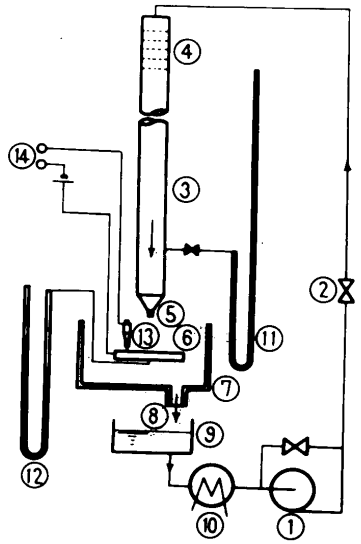

Fig.1 Flow system

In the experiments for heat transfer the heating surface was composed of a stainless steel plate whose dimensions were 80 mm in width, 300 mm in length and 0.1 mm in thickness attached to a bakelite plate whose diameter was 500 mm. This stainless steel plate was heated by alternate current passing directly through it. It was difficult to measure the surface temperature of the heating plate. In the experiments the backside temperature of the heating plate was measured and converted by means of calculated corrections. Two correction terms were found when the test plate was considered as a slab with internal heat generation and an insulated backside ; one term occurred because of heat conduction normal to the surface and the other term did because of heat conduction parallel to the surface. But due to the extreme thickness of the test plate, the value of parallel conduction term was negligible. Hence the surface temperature was found to be

$$t_w = t_w' - q\delta_p/2\lambda_s$$

The backside temperature was measured by C-A thermocouples whose diameters were 0.05 mm. Fourteen thermocouples were set at intervals of 20 mm. Continuous wall temperature distribution was measured by traversing the heating plate 20 mm relative to the jet.

Experimental conditions were as follows : inner diameter of the nozzle 5.7 ,

10, 17 mm ; flow velocity 1~6 m/s;and flow rate 50~500 cc/s.

2.2 Experiments with two equal jets

The heating surface used in the experiments are shown in Fig. 2. Heating method was the same as the prescribed one. The heating surface was traversed at a constant speed of about 2 cm/min by synchronous motor. (Preliminary experiments revealed that this traversing speed was low enough for the measured temperature to coincide with that at steady state.) Two thermocouples were set at interval of 70 mm for temperature measurement. Continuous temperature distribution of the heating plate was measured by traversing the heating surface 80 mm. Recording of the temperature was done by X-T recorder and temperature at any point could be known from the value at corresponding time. Temperature distributions were mainly measured along the line connecting the centers of each jet.

Experimental conditions were as follows : nozzle diameter 4.5, 7.0 and 10 mm; distance between two jets 20, 40, 80 and 120 mm ; and flow rate per one jet 25~250 cc/s.

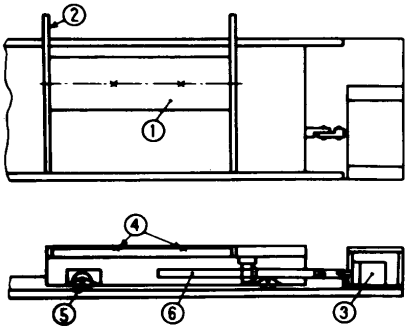

1 Heating surface 4 Thermocouples
2 Electrode 5 Wheel
3 Synchronous motor 6 Screw

Fig. 2 Heating surface

3. Experimental results and discussion

3.1 Thickness of water film

The thickness of the water film which was formed by an impinging jet on the horizontal plane was measured. The measured results are shown in Fig. 3. When Re_{ri} is the same, δ/r_i depends only on (r/r_i) regardless of the nozzle diameter.

Watson analysed approximately this flow by using the momentum integral equation.[2] He showed that for laminar flow the dimensionless film thickness, $\delta^*=(\delta/r_i)\times Re_i^{1/3}$,was a function of the dimensionless radius, $r^*=(r/r_i)Re_i^{-1/3}$;and for turbulent flow $(\delta/r_i)Re_i^{1/9}$,was a function of$(r/r_i)\times Re_i^{-1/9}$. The measured results of the film thickness shown in Fig. 3 were correlated by both functional relations. The correlation for turbulent flow,$(\delta/r_i)Re_i^{1/9}$ vs.$(r/r_i)Re_i^{-1/9}$ was not good.The correlation for laminar flow,$(\delta/r_i)Re_i^{1/3}$ vs. $(r/r_i)Re_i^{-1/3}$ was good as shown in Fig. 4.

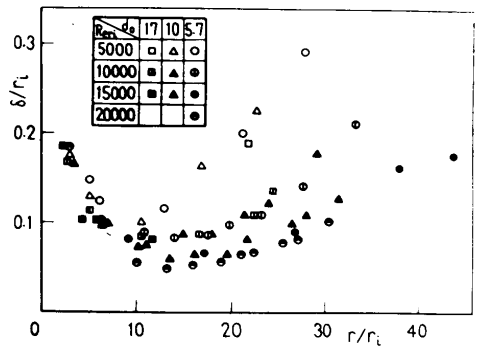

Fig. 3 Measured film thickness

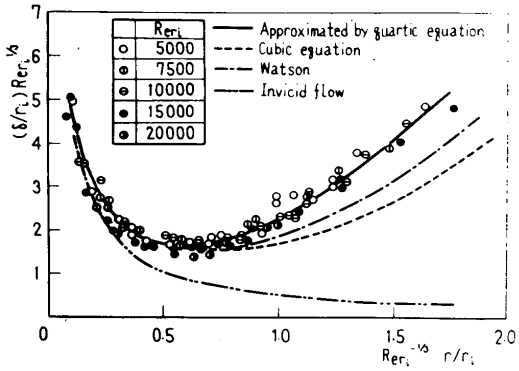

Fig. 4 Correlation of film thickness

In Fig. 4 Watson's theoretical correlation for laminar flow is also shown. As an approximeted velocity profile for the momentum integral equation,Watson used a similar velocity profile,which was exact at the developed film flow region,throughout the whole flow region.To know how much error in estimation of the film thickness was caused due to error of approximated velocity profile, the film thickness was calculated by the momentum integral equation using two approximate velocity profiles. The one approximates the velocity profile by the cubic equation, $f=-(1/2)\eta^3+(3/2)\eta$, and the other approximates by the quartic equation, $f=2\eta-2\eta^3+\eta^4$, where f is the nondimensional similar velocity profile and η is the nondimensional length, and the definitions of these nondimensional variables are described later. They are the approximate velocity profiles often used in hydrodynamical calculations.

In this film flow the boundary layer thickness increases along the wall from the stagnation point. But within a certain radius r_a the boundary layer is thinner than the film. In this region the definitions of f and η are as follows; $\eta=y/\delta_b$ and at $\eta<1$ the prescribed two functions are used for f and at $\eta>1$ $f=1$. At $r>r_a$the whole flow passes through the boundary layer. In this region $\eta=y/\delta$ and $f=u/u_s$. These calculated results are also shown in Fig. 4. Calculated results agree well with each other when $r^*=(r/r_i)Re_i^{-1/3}$is small. But when r^* becomes large, discrepancy among these calculated results becomes large. The reason why calculated results agree with each other at small r^* is that the boundary layer thickness is small com-

pared with the film thickness and error of approximated velocity profile does not come out directly. On the other hand at the developed film flow region, errors of approximated velocity profile are accumulated. Therefore film thickness estimated by using the momentum integral equation is not very accurate. Thus the calculated film thickness using the quartic equation, $f=2\eta-2\eta^3+\eta^4$, as the approximated velocity profile agrees well with the measured thickness. The calculated results are as follows;

$$\delta^* = 1.01r^{*1/2}-0.5/r^* \quad \text{at } r^* < r_a^* \quad (1)$$

$$\delta^* = 1.41r^{*2}- 0.315/r^* \quad \text{at } r^* > r_a^* \quad (2)$$

where $r^*=Re_i^{-1/3}(r/r_i)$, $\delta^*=(\delta/r_i)Re_i^{1/3}$ and r_a^* is dimensionless radius where the boundary layer thickness equals to the film thickness and

$$r_a^* = 0.212$$

It is known from the experimental results of heat transfer that the laminar boundary layer grows from the stagnation point and the turbulent transition occurs in this film flow.[1] But at the developed film flow region flow characteristics are determined by the film Reynolds number Re_δ. Re_δ decreases with an increase of radius measured from stagnation point because $Re_\delta = u_m\delta/\nu = Q/2\pi r\nu$. Therefore the turbulent flow becomes again a laminar film flow as the radius increases. Measured results shown in Fig. 4 reveal that the turbulent region is relatively narrow.

Measured thicknesses of the water film which is formed by the impinging jet ejected from a long nozzle whose length is $50d_o$ are shown in Fig.5. In this figure equations (1) and (2) are shown by a solid line. The measured values can be correlated also by the functional relation for laminar flow, but they are larger than the values estimated from equations (1) and (2). The reason why the equations (1) and (2) underestimate is considered to lie in the velocity at the center of the jet is greater than the mean velocity. Nagai et al. measured the film thickness in this condition and proposed an empirical equation for the film thickness, assuming that the film changes to a laminar flow from a turbulent flow.[3] The experimental results shown in Fig. 5 are compared with Nagai's empirical equation in Fig. 6. It is known that Nagai's equation overestimates.

3.2 Hydraulic jump

3.2.1 Types and radius of jump

The radial location of the hydraulic jump is changed by changing the height of the weir which is set around the test plate. Various types of the jump were observed. Fig. 7 shows sketches of these types. These types can be classified according to the film Froude number of the incoming flow whose representative length is the film thickness, calculated from eqs. (2) and (1), and representative velocity is the mean of the film flow. The classification according to the Froude

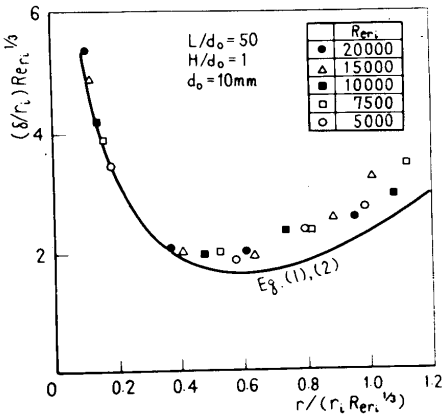

Fig. 5 Measured film thickness

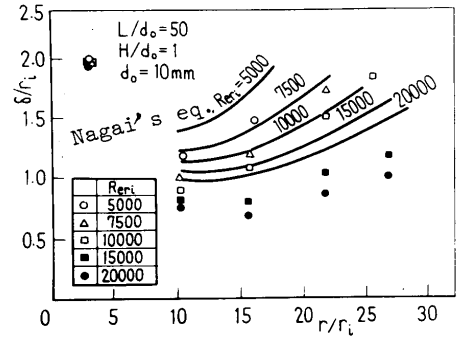

Fig. 6 Comparison with Nagai's empirical equation

number is as follows ;

(1) Fr<2 water surface is smooth and transparent. The jump is stable.

(2) 2<Fr<7 the jump becomes S-shaped. Ripples are observed at the water surface and the surface becomes opaque.

(3) 7<Fr<15 the jump becomes round and its width is very narrow.

(4) 15<Fr the front face of the hydraulic jump collapses and air is caught up in the water. The jump is unstable.

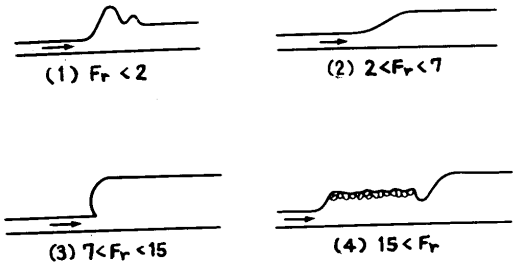

Fig. 7 Types of hydraulic jump

As shown in Fig. 7 the jump has a certain length. In Fig. 8 the experimental data on the length of the jump are plotted against Fr. At Fr<15 the length decreases as Fr increases, but at Fr≈15 the length increases suddenly. These types of the jump are different from those described in a textbook on the open channel hydraulics.[5]

Relation between radius of jump and flow rate of jet is shown in Fig. 9. The radius is evaluated at the centre of the

jump. Fig. 9 shows that the radius of the jump is independent of the nozzle diameter and depends on the height of the weir. At hydraulic jump the principle of momentum conservation can be applied. To calculate the radius of the jump a simple model was used. The model is as follows ; the jump has no length and the film thickness increases suddenly from δ_1 to δ_2 at the radius r_j. The condition to be applied at the jump is that the thrust of the pressure is equal to the rate at which momentum is destroyed. This condition is

$$\int_0^{\delta_1} u^2 dy - \int_0^{\delta_2} u^2 dy = \frac{g}{2}(\delta_2^2 - \delta_1^2) \qquad (3)$$

The radius of jump can be calculated from eq. (3). But the radius can be calculated more easily by introducing two more assumptions. The one is that $\delta_2 >> \delta_1$. The other is that the velocity after jump is uniform over the film thickness because the flow is reconstructed by the jump. Using these two assumptions at the developed film flow region,

$$u = u_s f(\eta) \ , \ \eta = y/\delta_1 \quad \text{and}$$

$$Q = 2\pi r_j \delta_1 u_s \int_0^1 f d\eta = 2\pi r_j \delta_2 U_m$$

When these equations are introduced into eq. (3)

$$r_j = \frac{Q}{\sqrt{2g}\,\pi\delta_2}\sqrt{\frac{K_2}{K_1^2}\frac{1}{\delta_1} - \frac{1}{\delta_2}} \qquad (4)$$

where

$$K_1 = \int_0^1 f\,d\eta \quad \text{and} \quad K_2 = \int_0^1 f^2 d\eta$$

The jumps observed in the experiments almost occurred at the developed film flow region. Then the radii of the jump are compared with eq. (4). In the calculation of r_j, δ_1 is calculated from eq.(2), δ_2 is measured and $f = 2\eta - 2\eta^3 + \eta^4$. The results are shown in Fig. 10. Agreement between the measured and the calculated radius is good except at large radius. The reason why the measured radius is larger than the calculated one at large radius is considered to lie in that at large radius the gravity force influences the film thickness of jet flow.

Kurihara[6] and Tani[7] regarded the hydraulic jump as a separation of the flow induced by the gravitational pressure gradient due to the variation in height of the free surface. In Fig. 11 calculated radii from the approximated equation proposed by Kurihara are compared with our experimental results which were measured without the weir. The calculated results agree qualitatively with experimental results, but quantitatively discrepancies between the calculated and the experimented results are large. It is observed that in the experiments the radius of the jump became larger by the removal of the water after the jump with hand. These results show that the jump does not occur as a result of the separation of the flow induced by the gravitational pressure gradient mentioned by Kurihara and Tani.

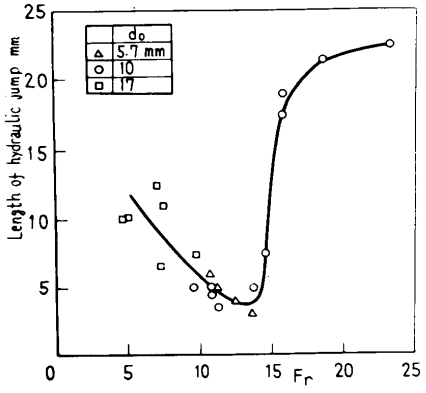

Fig. 8 Length of hydraulic jump

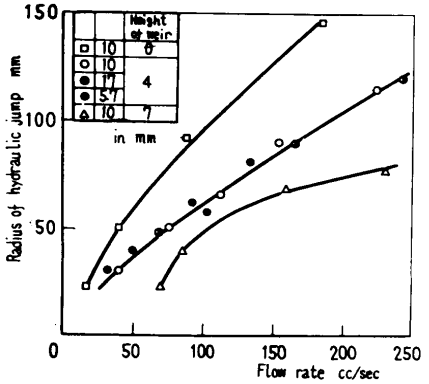

Fig. 9 Radius of hydraulic jump

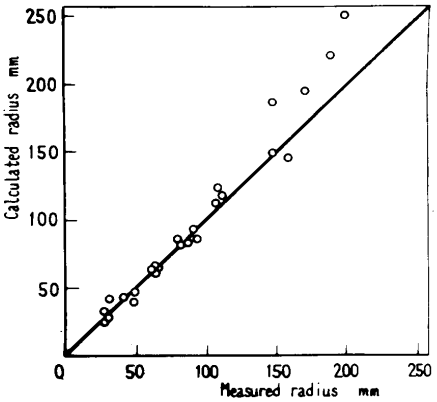

Fig. 10 Comparison between calculated and measured radii of jump

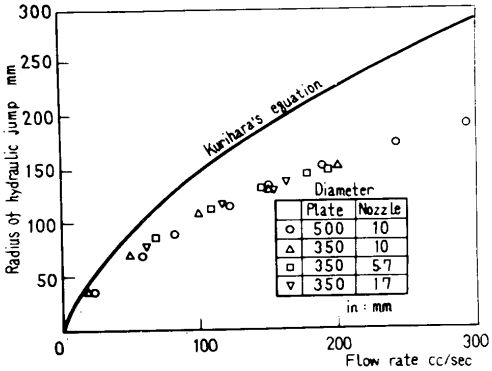

Fig. 11 Comparison with Kurihara's equation

3.2.2 Improvement of heat transfer characteristics by hydraulic jump

In the jump it is expected that heat transfer characteristics change due to the mixing motion of the water. To examine the influence of the jump on the heat transfer characteristics the changes of the heat transfer coefficient after the jump were measured. An example of radial change of the heat transfer coefficient when the radius of the jump is changed under the same jet conditions is shown in Fig. 12. The radial change of the heat transfer coefficients with no jump, corresponding to 6 in Fig. 12, has a minimum and a maximum value. The minimum heat transfer coefficient corresponds to the point where turbulent transition begins.

The changes of the heat transfer characteristics by the jump are divided into two groups; the one in which the heat transfer coefficients increase after jump and the other in which the heat transfer coefficients decrease after jump. Under the other experimental conditions the two groups were observed also. Inspection of these results showed that only the jumps before turbulent transition improved the heat transfer characteristics.

The flow in the jump is similar to the separation flow. In the heat transfer coefficients near the separation point of a circular cylinder, the same behaviors are observed[8] as in the jump ; at laminar separation the heat transfer coefficients increase locally, but at turbulent separation they decrease.

In Fig. 13 two examples of radial variation in wall temperature are shown; (a) is the case that heat transfer coefficients increase in the jump and (b) is the case that they decrease. Generally speaking, after the jump the wall temperature fluctuates by large eddies, but when the heat transfer coefficients increase in the jump region the wall temperature does not so much fluctuate at a distance from the jump.

The reason why heat transfer coefficients increase by the jump caused in

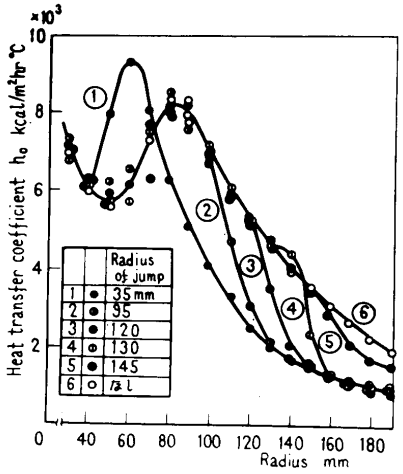

Fig. 12 Change of heat transfer characteristics by hydraulic jump

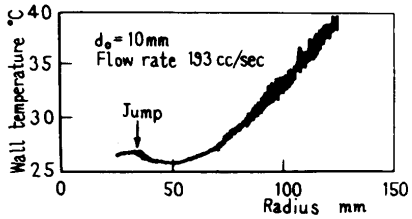

(a) when heat transfer coefficient increases after jump

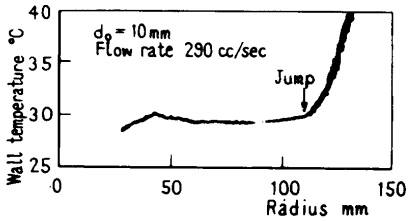

(b) When heat transfer coefficient decreases after jump

Fig. 13 Change of wall temperature by hydraulic jump

laminar flow is considered to lie in that transition to turbulent flow is promoted by the jump. But increase in the heat transfer coefficients is local phenomenon and at a large distance from the jump the coefficients become lower than those of the jet flow. It seems that the types of the jet flow. It seems that the types of the jump shown in Fig. 7, have no decisive influence on the types of heat transfer characteristics.

3.3 Interfering films of two equal jets

The coordinate system in the experiments is shown in Fig. 14. The point O is stagnation point produced by impinging two equal jets, A and B. We call this stagnation point the secondary stagnation point for convenience sake. The coordinate system is chosen such that the point O is the

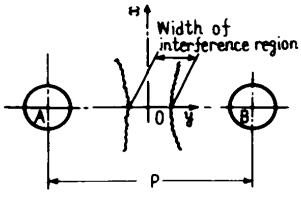

Fig. 14 Coordinates system for two jets

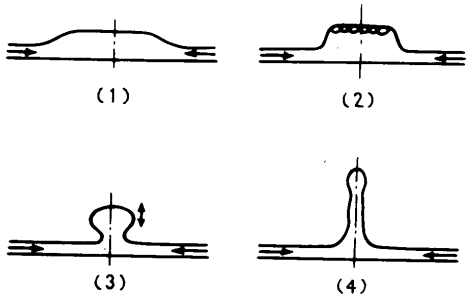

Fig. 15 Types of flow in the interference region

origin and OA is y-axis. Heat transfer characteristics were studied mainly along the line OA. The types of the flow change with the condition of jets. They are divided into four types as shown in Fig. 15. They are as follows:

(1) The jump is weak and wide. Standing up of the water is small.

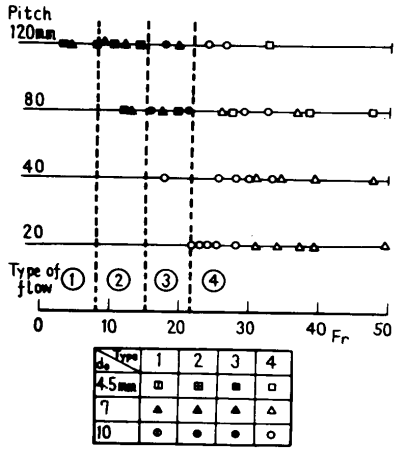

Fig. 16 Types of flow classified by Froude number

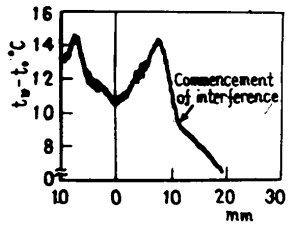

Type (1)
P =120 mm
d_o=4.5 mm
Q =45.1 cc/s
(per one jet)
Fr=3.37

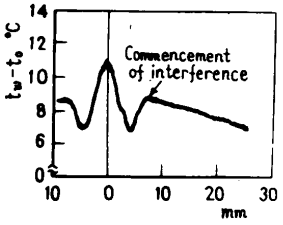

Type (2)
P =120 mm
d_o=7.0 mm
Q =74.3 cc/s
Fr=8.48

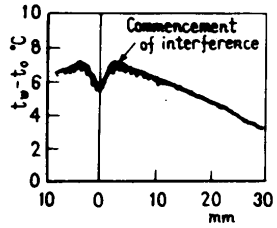

Type (3)
P =80 mm
d_o=7.0 mm
Q =72.2
Fr=20.7

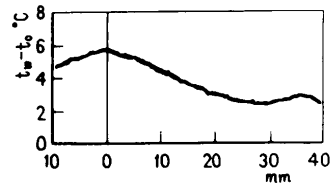

Type (4)
P =120 mm
d_o=4.5 mm
Q =88.0 cc/s
Fr=32.8

Fig. 17 Types of heat transfer characteristics

(2) Air bubbles are caught up in the jump and the water rises in round form.

(3) Air bubbles disappear and the water rises and falls alternately.

(4) The water stands up continuously.

These types are classified according to the Froude number evaluated at the secondary stagnation point. The results are shown in Fig. 16.

In the vicinity of the secondary stagnation point heat transfer characteristics also change according to jets conditions. The changes of the heat transfer characteristics are divided into four types. The representative examples of these types are shown in Fig. 17. In this figure the recorded wall temperatures are shown in order to show the phenomenon precisely. As the experiments are performed under the condition of uniform heat flux, the maximum wall temperature corresponds to the minimum heat transfer coefficient and the minimum wall temperature corresponds to the maximum heat transfer coefficient. These four types are as follows:

(1) The wall temperature falls suddenly after interference of the water film, but after a little distance it decreases and takes a minimum value at the secondary stagnation point.

(2) The wall temperature falls suddenly after interference of the water film, but after a little distance it rises and takes a maximum value at the secondary stagnation point.

(3) The wall temperature falls after interference and takes a minimum value at the secondary stagnation point.

(4) There is no change in wall temperature.

In Fig. 18 the types of the heat transfer characteristics are plotted against the film Froude number evaluated at the secondary stagnation point. The types of heat transfer characteristics can be classified by the Froude number excepting the distinction between (3) and (4). In this

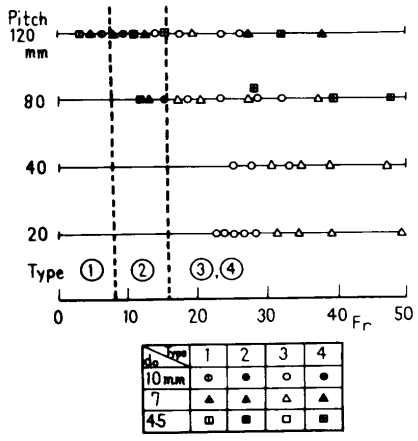

Fig. 18 Types of heat transfer characteristics classified by Froude number

figure the critical Froude numbers are shown by dotted lines.

These critical Froude numbers coincide with those of the flow field. Inspecting all experimental data, it is known that the heat transfer characteristics show the type (4) when interference of the films occurs after turbulent transition. Namely the distinction between type (3) and (4) can be made by the Reynolds number Rer evaluated at the secondary stagnation point. If this Rer is smaller than the critical Reynolds number Recr, the type of the heat transfer characteristics is (3). In the experiments the critical Reynolds number was about 2×10^5. Width of the interference region defined in Fig. 14 is shown in Fig. 19. At Fr<15 the width decreases as Fr increases, but at Fr>15 the width changes little. The types of hydrodynamic and heat transfer characteristics are summarized in Table 1.

The cooling power of two equal jets over the whole plane can be estimated by the power of a single jet if the conditions of jets are corresponding to the type (4) of heat transfer. If the conditions of jets are corresponding to the type (3) of heat transfer, the cooling power of two jets over the whole plane is storonger than the one estimated by the power of a single jet. In Fig. 20 measured heat transfer coefficients over the whole plane are shown. The experimental results verify the above-mentioned matter.

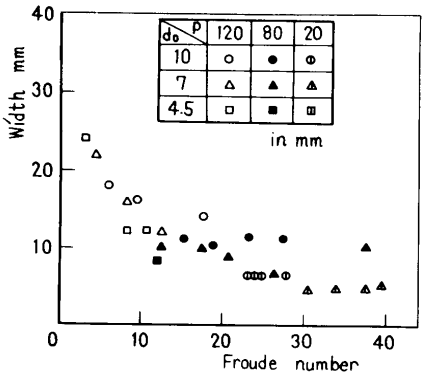

Fig. 19 Width of interference region

Table 1 Classification of hydrodynamic and heat transfer characteristics

Fr	Rer	Types of flow	Types of heat transfer
Fr<8		(1)	(1)
8<Fr<15		(2)	(2)
15<Fr<22	Rer<Recr	(3)	(3)
	Rer>Recr	(3)	(4)
22<Fr	Rer<Recr	(4)	(3)
	Rer>Recr	(4)	(4)

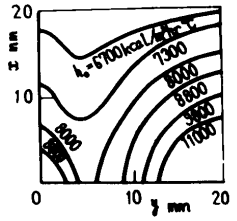

(a) Type (3) of heat transfer characteristics

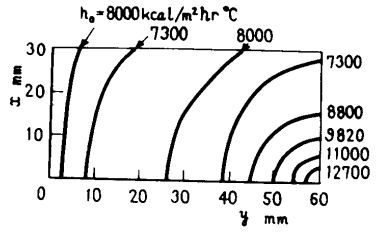

(b) Type (4) of heat transfer characteristics

Fig. 20 Heat transfer coefficient over the whole plane

4. Conclusions

(1) Measured thickness of the water film, which is formed by an impinging jet, agree well with the calculated results from the momentum integral equation by using the approximate velocity profile of the quartic equation. Watson's equation underestimates and Nagai's equation overestimates the film thickness.

(2) The mean radius of hydraulic jump can be calculated from the principle of momentum conservation by using a simple model.

(3) The types of flow in the interference region of film flow change with the film Froude number.

(4) Heat transfer characteristics in the interference of film flow change with the film Froude number and the Reynolds number whose representative length is the radius measured from the center of the jet.

References

(1) Ishigai,S.,et al.Preprint Japan Soc. Mech.Engrs.(in Japanese),No.714-7(1971-3),81.
(2) Watson,E.J.,J.Fluid Mech.,20-3(1964-11),481.
(3) Nagai,I.,et al.,Trans.Japan Soc.Mech. Engrs.(in Japanese),21-104(1955),481.
(4) Nagai,I.,et al.,Trans.Japan Soc.Mech. Engrs.(in Japanese),23-132(1957),609.
(5) Chow,V.,Open Channel Hydraulics(1959),395,MacGraw Hill.
(6) Tani,I.,J.Phys.Soc.Japan,(1948),212.
(7) Kurihara,M., Report of the Reseach Institute for Fluid Engineering,Kyusyu Imperial University,3-2(1946),11.
(8) Giet,W.H.,J.Aeron.Sci.,18-11(1951-11),725.